Optical Coherence Tomography Angiography Features of Choroidal Nevi

Susana Henriques[1]; Rita Basto[1]; Joana Roque[1]; Inês Coutinho[2]; Luísa Colaço[2]; Filomena Pinto[3]; Filomena Silva[4]; Isabel Prieto[5]
[1] Interna de Formação Específica, Hospital Professor Doutor Fernando Fonseca
[2] Assistente Hospitalar, Hospital Professor Doutor Fernando Fonseca
[3] Assistente Hospitalar Graduado, Centro Hospitalar Lisboa Norte – Hospital de Santa Maria
[4] Chefe de Serviço, Hospital Professor Doutor Fernando Fonseca
[5] Chefe de Serviço, Diretora de Serviço, Hospital Professor Doutor Fernando Fonseca

ABSTRACT

Purpose: To describe the imaging features of choroidal nevi using optical coherence tomography angiography (OCT-A) and optical coherence tomography with enhanced depth imaging (EDI-OCT).

Material and Methods: Retrospective case series of patients with choroidal nevi. The tumor and overlying retina structural features were analyzed with EDI-OCT. The OCT-A images were evaluated for vascular changes at the level of the retinal plexus, outer retina, choriocapillaris and choroid. Statistical analysis was performed using IBM SPSS Statistics.

Results and Discussion: A total of 21 patients (73% female) were included, with a mean age of 55±10 years old. The mean tumor thickness was 359±42 µm and the mean largest basal diameter was 3089±261µm. Only 27% of the nevi had their epicenter in the macula. Ultrasonography (US) showed a solid flat lesion with high reflectivity. With EDI-OCT all lesions appeared as a highly reflective band within the choriocapillaris with posterior shadowing. Most nevi had drusen (67%) and 25% had drusenoid pigment epithelium detachment. Chronic changes in the retina were found in 52% and subretinal fluid in 16%. On OCT-A, no changes were noted, except for a neovascular membrane, a polypoidal vasculopathy and 4 cases that demonstrated flow under the detached retinal pigment epithelium (RPE). At the level of the choriocapillaris (CC), on OCT-A, the lesions demonstrated variable reflectivity.

Conclusion: Our work demonstrated that OCT-A may be a useful and safe complementary imaging technique in the diagnosis of vascular complications associated to small stable nevi. The identification of features typical of neovascularization is crucial in order to establish a treatment strategy, avoiding further visual impairment.

Key Words: choroidal nevus, retinal epithelium detachment, choroidal neovascularization, polypoidal choroidal vasculopathy, optical coherence tomography, optical coherence tomography angiography

INTRODUCTION

Choroidal nevus (CN) is defined by the Collaborative Ocular Melanoma Study (COMS) as a benign melanocytic tumor less than 5 mm and 1 mm in largest basal diameter and in height, respectively,[1] but Shields and al. in a large study with 3422 nevi showed an increased mean thickness of 1,5 mm.[2] Clinical prevalence varies from 4.2% to 7.9% depending on the study population, study criteria, and evaluation method.[1,3] The typical CN appears as a subretinal flat grey to brown lesion often associated with drusen. Most nevi are asymptomatic and discovered on a routine examination. However, when located in the macular region they may cause visual impairment due to external retina and/or retinal pigment epithelium (RPE) disruption or atrophy, subretinal fluid and RPE detachment (PED). Although these features are secondary to chronic retinal and RPE degeneration or choroidal neovascularization (CNV), they may be confused with malignant signs.[2] Imaging modalities for evaluation of CN include US, fundus autofluorescence (FAF), and spectral domain optical coherence tomography (SD-OCT). Fluorescein angiography (FA) is occasionally employed to detect multifocal pinpoint leaks or CNV. Recently, OCT angiography (OCT-A) has been applied to the study of retinal and choroidal vasculature in several macular diseases including choroidal tumors.[4,5] OCT-A has the ability to separately evaluate superficial and deep retinal vascular plexus, choriocapillaris (CC), and choroid, with no need for dye injection, but also the disadvantage of being unable to detect alterations in vascular permeability or leakage, as FA does.[6]

The aim of this study was to describe structural and vascular findings in stable choroidal nevi, using SD-OCT and OCT-A.

MATERIAL AND METHODS

Inclusion criteria and data collection

In this retrospective study we reviewed the records of 26 patients with presumed CN, based on clinical and ultrasound features. Inclusion criteria for the study included patients with macular and extramacular choroidal melanocytic lesions with less than 1.5 mm in thickness (initially measured by US and according to mean thickness described by Shields), accessible to OCT-A. The exclusion criteria were a history of microvascular abnormalities, age-related macular degeneration (AMD), glaucoma and intraocular inflammation. We selected 21 patients who had undergone a complete ocular examination including best corrected visual acuity (BCVA), intraocular pressure (IOP), slit-lamp examination and dilated fundus examination. Multimodal imaging with fundus color photography, US, EDI-OCT, FAF and OCT-A had also been performed in all patients. When clinically indicated, some patients had undergone FA and indocyanine green angiography (ICGA). Information on patient characteristics, including demographics, medical/ocular history and referral symptoms, were analyzed from the records. Structural features of the tumor and retina were extracted from multimodal imaging. We defined the macula according to ETDRS grid (3 mm from the foveola) and the location of the tumor was defined as macular or extramacular, according to its epicenter.

Spectral Domain Optical Coherence Tomography Acquisition and Analysis

Spectral-domain OCT was performed with a Heidelberg Spectralis HRA OCT system (Spectralis, Heidelberg Engineering, Germany) with acquisition and analysis software version 5.3.4.0 with automated EDI. This instrument operates at 870 nm with an axial resolution of 3.5 µm/pixel and a scan speed of 40 000 A-scans per second. Volume scans, horizontal and vertical EDI-scans with 100 frames each, centered on the lesion were obtained to evaluate retinal and choroidal features. Horizontal and vertical diameters were calculated based on the presence of a shadow cone created by the lesion's lateral borders. Tumor thickness was measured between the RPE and the innermost hyperreflective edge of the sclera. In cases where the this edge was not clearly visible due to posterior shadowing, we used the method described by Shields et al:[7] curve 1 was automatically defined at the level of the RPE and curve 2 was manually positioned at the closest location to the nevus where inner sclera was still visible, and auto-segmentation produced the expected curve (Fig.1A). Tumor features were analyzed for thickness and largest tumor diameter (in µm), subretinal fluid (SRF), orange pigment, cystoid macular edema, outer retina and RPE changes and overlying drusen or PED. Drusenoid PEDs were defined as lobular detachments of the RPE with underlying homogenous, hyperreflective material, measuring at least 350 µm in the narrowest

diameter. Presumed vascularized PEDs were defined as detachments of the RPE with less-defined margins, irregular shape and underlying heterogeneous, hyperreflective material.

OCT Angiography Acquisition and Analysis

OCT-A was performed using a Heidelberg Spectralis HRA OCT system with Angiography Module (Spectralis, Heidelberg Engineering, Germany). This instrument operates with a transversal resolution from 5.7 to 11.4 µm and an axial resolution of 3.9 µm/pixel, which allows for segmentation of retinal vascular plexus, CC and choroid. The volume scans provide a three-dimensional cube of data that includes structural OCT and OCT-A images. *En face* images and section images are combined into a *fusion* image to provide a correlation between structural and flow information. Flow signals are displayed in yellow and can be interpreted as vessels. The images were captured with the retina protocol with raster scan patterns of 3x3 mm (512 A-scans per B-scan) or 6x6 mm (245 A-scans per B-scan) centered on the lesion. Low quality scans due to low signal, movement or positioning errors, were repeated or excluded. The OCT-A images were semi-automatically segmented and evaluated for changes at the level of the retinal plexus, the CC and the choroid. Segmentation errors related to morpho-structural alterations of retinal layers and choroid, were avoided by viewing the segmentation contours in sequential OCT B-scans and manually correcting the slabs, especially at the level of the RPE and the CC/choroid. This time-consuming task is facilitated by Spectralis OCT-A, that provides a segmentation propagation tool, with which the correction of only a few scans lead to correction of compromised slabs of the entire volume.

The outer retina and RPE-Bruch's membrane are normally avascular and any flow in these layers could be interpreted as pathologic vascularization. In cases with macro drusen or drusenoid PEDs over the tumor, the RPE slabs were corrected in order to follow its new anatomical contour and avoid misinterpretations. In cross-section, the presence of a flow signal at the level of the outer retina or RPE was interpreted as intrinsic if there was no corresponding flow signal in the overlying inner retina at the same A-scan axis. A vascularized PED was suspected when a positive flow signal was detected underneath the PED on cross-sectional OCT-A and a tangle of vessels was seen on *en face* OCT-A, in the absence of motion and projection artifacts. At the level of the CC the images were examined for intrinsic flow and the lesion was considered isorreflective, hyporreflective or hyperreflective when compared with the surrounding normal vasculature.

Statistical Analysis

Analysis were performed with the use of IBM SPSS Statistics. Categorical variables are presented as frequencies and percentages and continuous variables as means and standard deviations or medians and interquartile ranges for variables with skewed distributions. Normal distribution was checked using Shapiro-Wilk test.

RESULTS

Baseline characteristics of patients and eyes analyzed:

In this study a total of 22 eyes with CN (21 patients) were included. The patients consisted of 6 men and 15 women aged between 42 and 82 years (55±10 years). The mean tumor thickness measured by OCT was 359±42 µm. With ultrasound, 15 (68%) nevi were flat and the remaining 7 (32%) presented as small lesions with less than 1.5 mm (1.2±0.1 mm) and high reflectivity (Fig. 1). The mean largest basal diameter was 3089±261 µm measured by EDI-OCT. Only 27% of the nevi had their epicenter located at the macula and 73% were extramacular. The foveola was involved by the CN in 3 eyes. Most of patients (81%) did not have symptoms related to the tumor.

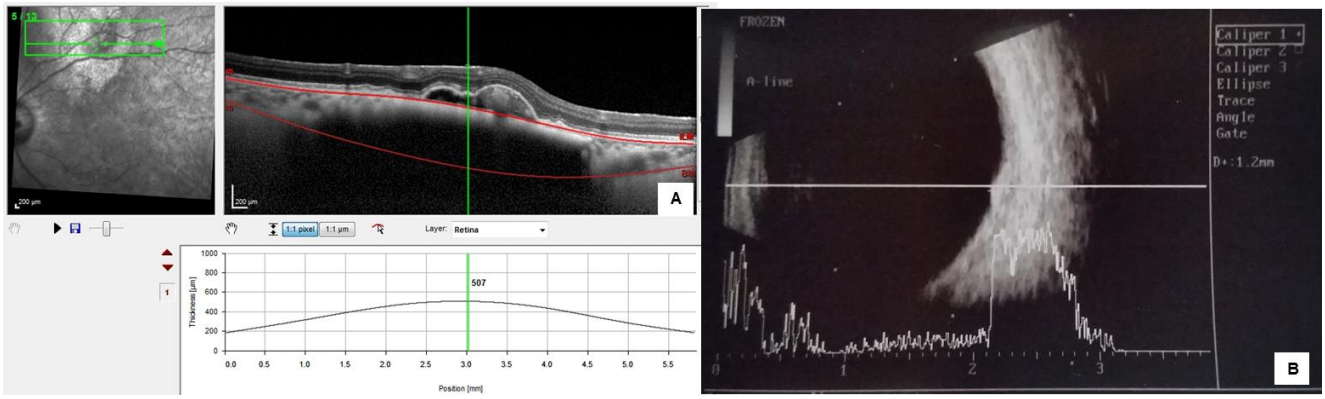

Figure 1 - Choroidal nevus thickness measured by EDI-OCT and ultrasound. (A) With EDI-OCT the internal and external boundaries are identified (retinal and scleral thickness is not included in the measurement). (B) With US, in these small high reflective lesions is not possible to separate the different structures (retina, PED, choroid and sclera) and the thickness of the nevus is overestimated (507 µm / 1200 µm).

On structural EDI-OCT (Fig. 2) all lesions appeared as a highly reflective band within the choriocapillaris with posterior shadowing. Chronic changes in the retina were found in 52% and subretinal fluid in 16%. Overlying RPE drusen were present in 67% and presumed drusenoid PEDs in 25%.

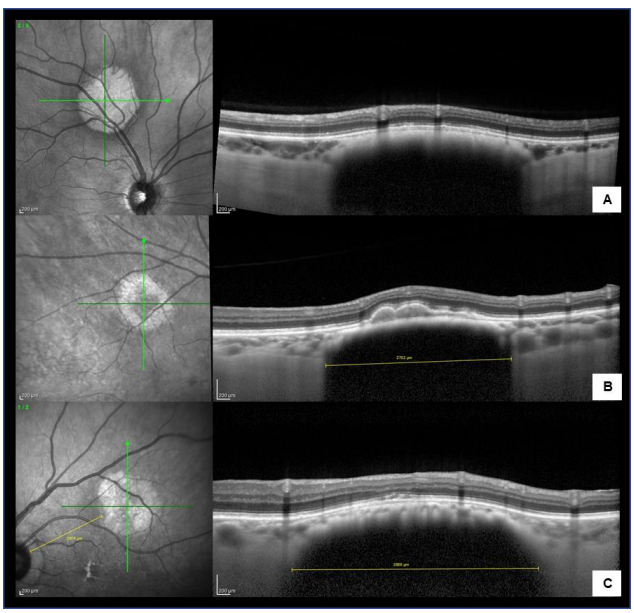

Figure 2 - EDI-OCT features of minimally elevated choroidal nevi presenting as a hyperreflective band with posterior shadowing associated to drusen of the RPE (A), pigment epithelium detachment (B) and outer retina changes (C).

On OCT-A the superficial and deep capillary plexus appeared undisturbed in all cases. Using custom slabs all nevi showed intact avascular complex (AC), except those associated to detached RPE. In fact, when a PED was present, the AC and the RPE appeared more susceptible to projection artifacts. However, after analyzing a *fusion* image of a slab passing through the PED it was possible to identify an intrinsic flow signal under the PED in 5 cases: a neovascular membrane was detected in 1 case (Fig. 3); a polypoid lesion and a branched vascular network (BVN) consistent with PCV was present in another case (Fig.5); two cases with tangled vascular structures might also be consistent with a PCV-like lesion (Fig. 4, 6); and in a case with an apparently vascularized flat PED without signs of activity, we were unable to clearly define the vascular complex (Fig. 7).

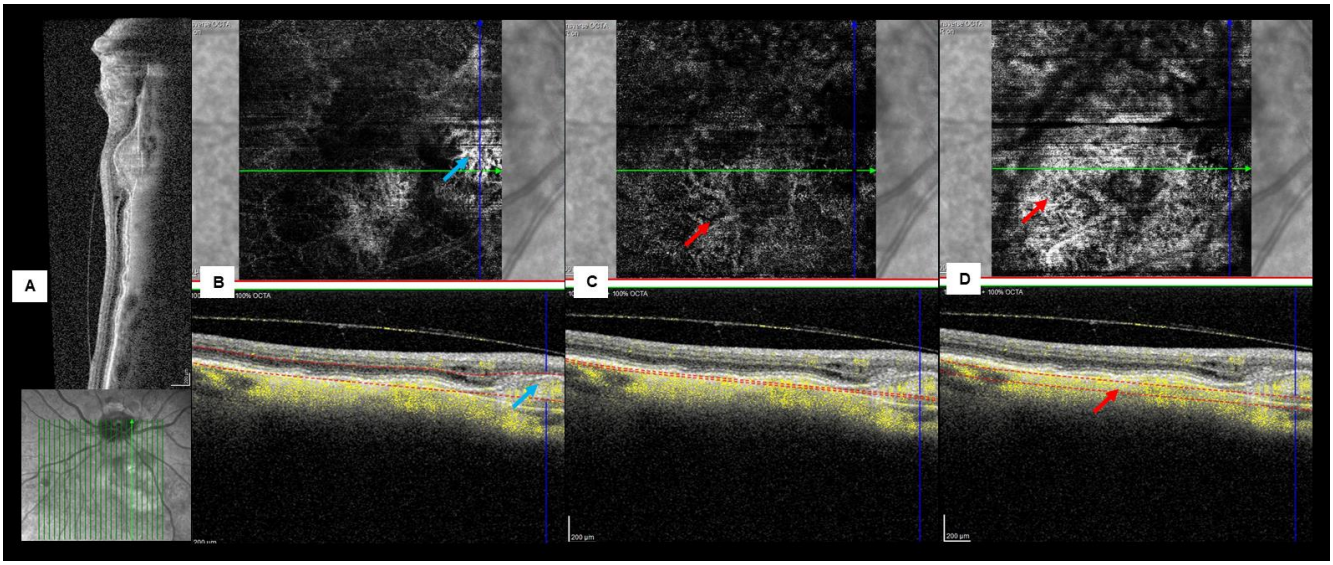

Figure 3 - Multimodal imaging of a left choroidal nevus nasal to the optic disc complicated by type 1 CNV. (A) Structural SD-OCT showing the nevus as a choroidal hyperreflective band with compression of CC and posterior shadowing. Intraretinal fluid and a fusiform lesion with heterogeneous reflectivity are seen over the nevus. (B) En face images and B-scan OCT-A of AC slab displaying a juxtapapilar type 1 CNV (blue arrow). A customized slab passing through the choriocapillaris (C) and the choroid (D) showing intrinsic vasculature (red arrow).

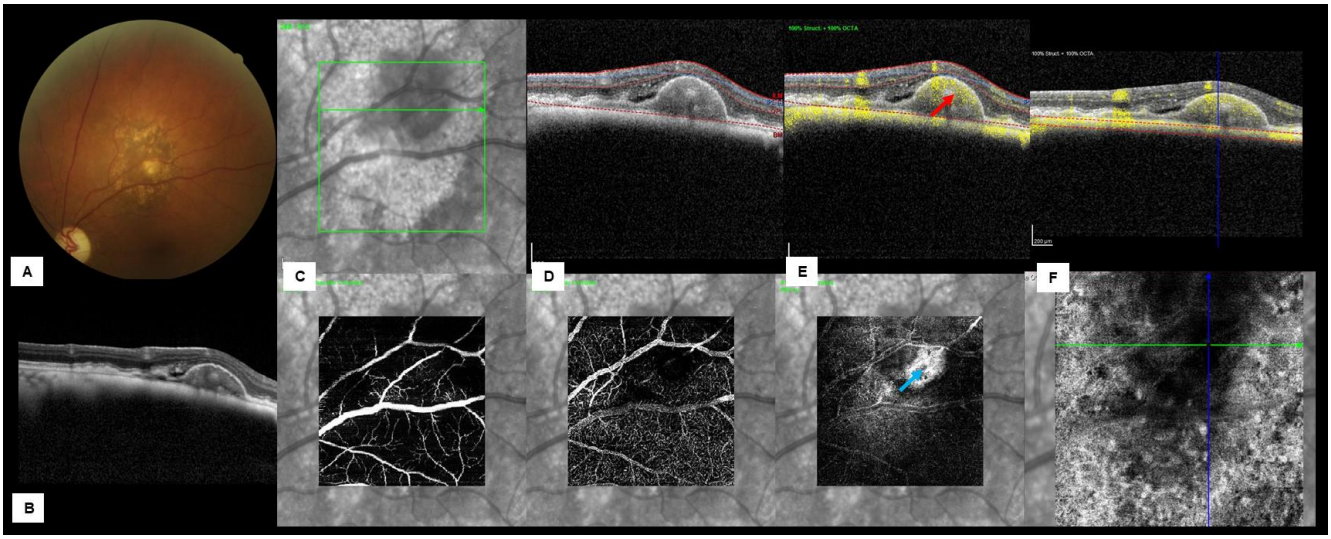

Figure 4 - Multimodal imaging of an extra-macular choroidal nevus with a vascularized PED. (A) Color fundus photograph showing a sub-retinal melanocytic lesion with multiple overlying drusen. (B) Structural EDI-OCT showing the nevus as a choroidal hyperreflective band with compression of CC and posterior shadowing. A large PED with heterogeneous reflectivity, double layer sign and SRF is evident over the nevus. B-scan OCT-A and en face images, showing normal superficial (C) and deep (D) retinal plexus. (E) At the level of the AC (from outer plexiform layer to Bruch membrane) a dome-shaped PED is seen demonstrating intrinsic flow (red arrow) on fusion image with tangled morphology on en face OCT-A (blue arrow). (F) At the level of the choroid the nevus is hyporreflective.

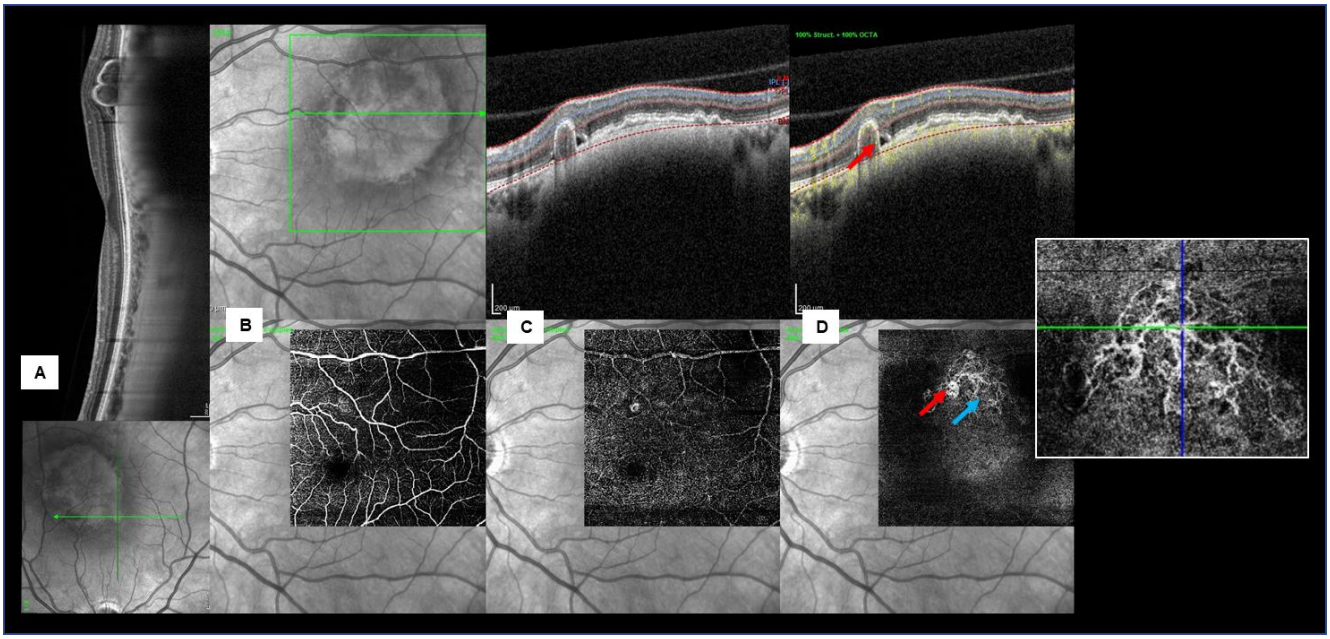

Figure 5 - Multimodal imaging of a patient with a left macular nevus, PCV and SRF. (A) Structural EDI-OCT showing the nevus as a choroidal hyperreflective band with compression of CC and posterior shadowing. A large notched PED with heterogeneous reflectivity is evident over the nevus. B-scan OCT-A and en face images, showing normal superficial (B) and deep (C) retinal plexus. (D) At the level of AC (from outer plexiform layer to Bruch membrane) a thumb-like polypoidal lesion demonstrating intrinsic flow on fusion image (red arrow) and a BVN on en face OCT-A (blue arrow) are seen.

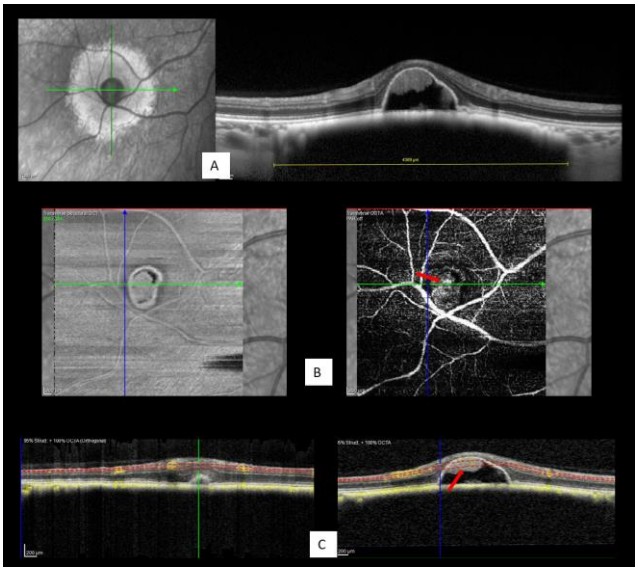

Figure 6 - Multimodal imaging of a right extra-macular choroidal nevus complicated by a vascularized PED. (A) Structural EDI-OCT showing the nevus as a minimally elevated choroidal hyperreflective band with compression of CC and posterior shadowing. A large PED with heterogeneous reflectivity, without SRF is evident over the nevus. En face images (B) and B-scan OCT-A of a customized slab passing through the PED (C) showing intrinsic flow on fusion image, with tangled morphology on en face OCT-A (red arrow).

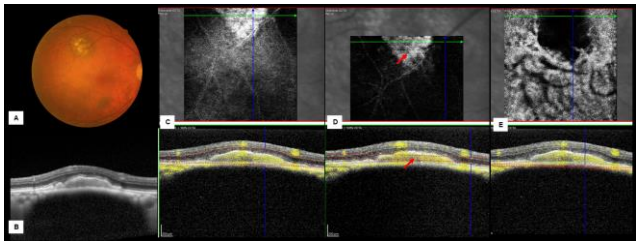

Figure 7 - Multimodal imaging of a right extra-macular choroidal nevus complicated by a vascularized PED. (A) Color fundus photograph showing a sub-retinal melanocytic lesion with multiple large overlying drusen. (B) Structural EDI-OCT showing the nevus as a minimally elevated choroidal hyperreflective band with compression of CC and posterior shadowing. A large irregular PED with homogeneous reflectivity, without SRF is evident over the nevus. En face images and B-scan OCT-A of AC slab (C) and a customized slab passing through the PED (D) showing intrinsic flow on fusion image and an ill-defined neovascularization (red arrow) on en face OCT-A (E) At the level of the choroid the nevus is hyporreflective.

We found that in our patients the acquisition of OCT-A images was relatively easy since most of the lesions were in the posterior pole or just outside the retinal vascular arcades and were less than 1.5 mm in thickness.

DISCUSSION

With our study we demonstrated that even small stable nevi may complicate with choroidal neovascularization.

We confirmed the importance of non-invasive multimodal imaging in the evaluation and monitoring of CN, especially OCT-A, which provide complementary vascular information, not obtained by structural exams like SD-OCT or US. We also demonstrated that with EDI-OCT, is possible not only to define retinal abnormalities induced by the presence of the tumor, but also to evaluate the dimensions of nevi, with more accuracy than with US, which is essential for follow-up.

In this analysis we evaluated 21 patients with CN (1 patient with bilateral disease) with thickness less than 1.5 mm. Thickness can be a vital feature in follow-up of suspicious lesions, small indeterminate choroidal lesions or even small melanoma (between 1-3 mm).[7] EDI-OCT enables precise measurement of small tumors, when compared to ultrasonography. Shields et al.[8] evaluated the characteristics of small choroidal melanoma using EDI-OCT and concluded that thickness was overestimated by 55% on ultrasonography. COMS group[9] established that ultrasonography overestimates choroidal melanoma thickness by at least 2 mm (compared with histopathologic analysis) in 10% of cases. Shah et al.[7] evaluated 51 nevi with a mean thickness of 685 μm by EDI-OCT compared with 1500 μm by ultrasonography. With US the precise identification of the inner and outer edges of the nevus is not accurate because the retina and/or the sclera may be included in the measurement. In our study we found a mean thickness difference of 620 μm between the EDI-OCT and ultrasonography measurements.

To better identify intrinsic morphologic features and risk factors for malignancy, multimodal imaging with EDI-OCT have been applied to the study of choroidal tumors. Shields et al[7,10] demonstrated that choroidal nevi usually displayed a smooth, dome-shaped topography with overlying retinal pigment epithelium alterations, drusen, and occasional subretinal cleft, a sign of photoreceptor loss. They also defined several factors predictive of transformation of choroidal nevus into melanoma.[11] Similarly, to previous structural imaging studies we found that all our lesions were easily detected and demarcated from the surrounding healthy tissue. On EDI-OCT they appeared as a highly reflective band within the choriocapillaris with posterior shadowing and compression of the CC. Overlying RPE drusen were present in the majority of the eyes. Drusen are extracellular deposits located between the RPE and Bruch's membrane and they have been commonly described in AMD.[12,13] Likewise, the presence of overlying drusen and RPE changes are also frequent in CN and have been considered signs of chronicity, with a probable relation to choriocapillaris insufficiency.[14] Curiously some of our nevi were associated to large drusen (pachydrusen) that recently, have been described in PCV, a disease included in the spectrum of pachycoroidopathy.[15] Similar to pachychoroid disease, where the presence of large choroidal vessels lead to the compression of medium choroidal vessels and CC,[16] we can speculate that the presence of a long-standing choroidal mass, with the consequent compression of the CC, may induce vascular impairment and explain the frequent location of such drusen over the nevi. In our study, drusenoid PEDs were also a common finding, seen on EDI-OCT as dome shaped elevations of the RPE with homogenous hyperreflective material underneath. In the setting of AMD, natural evolution for drusenoid PEDs varies from persistence to development of geographic atrophy or choroidal neovascularization (vascularized PEDs).[17] Likewise, we may expect a similar evolution to occur in long-standing nevi with large DEPs.

Although EDI-OCT enables the study of choroidal tumors and retinal changes induced by choroidal tumors, it does not permit visualization of choroidal vascularization. OCT-A on the other side, visualizes the retinal and choroidal circulation without the injection of dye. With this technique it is possible to identify normal and abnormal vascular features associated to the mass lesion and the effects over the surrounding tissues. There have been several reports showing the development of CNV secondary to stable nevi.[2,18–20] It seems that long-standing RPE changes and PED may lead to disruption of the Bruch's membrane and subsequent development of type 1 neovascular membrane which can evolve into BVN with polypoid lesions.[21] Confirmation of neovascularization is typically performed with conventional angiography with fluorescein and/or indocyanine green, providing information on leakage or pooling related to abnormal vascular permeability. However, with OCT-A, data are depicted in three dimensions, which allows for more precise axial localization of *in vivo* imaging of CNV size, shape and location.[22,23] The recognition of the vascular features typical of neovascularization has additional importance when analyzing CN, as the associated subretinal fluid can be easily misinterpreted as a sign of malignant transformation into melanoma.[23] Some studies have showed the presence of CNV in association to CN,

using OCT-A. Pellegrini et al.[23] described the features of CNV associated with 11 CN and concluded that OCT-A revealed the CNV in all cases. Toledo et al.[5] studied the microcirculation patterns of 55 choroidal nevi that were described mainly as hyperreflective and found neovascular membrane in 16.3%. Arumi et al.[24] described the imaging features of 18 CN and depicted a neovascular membrane in one case (6%). In recent years some cases of PCV secondary to nevus have also been reported,[25–28] but few have described OCT-A findings.[23] PCV is characterized by BVN and polyp-like aneurysmal dilations, that may cause serosanguinous PEDs,[29,30] but the occurrence of quiescent forms may explain the fact that this vasculopathy is often underdiagnosed.

In our study, using OCT-A, we were able to clearly define 1 case of CNV appearing as a round sea-fan. Our results also documented 1 case where OCT-A clearly depicted features consistent with of a PCV lesion (polyps and a peaked PED connected to a flat irregular PED) and 2 cases with subretinal fluid and a tangled vascular complex in close relation to PEDs, whose morphology might be consistent with a PCV lesion. Based on structural OCT, polypoidal lesions can be suspected in the presence of multiple PEDs, peaked or notched PEDs and polyp lumens adherent to the underside of the PED.[30–32] Although characterization of PCV using OCT-A is not ideal, BVN may be visualized as hyperflow structures with different morphologic patterns (sea-fan, tangled and Medusa head) and polyps may be identified as hypoflow round structures or as hyperflow lesions with a surrounding hypointense halo.[30,33,34] However, if their blood flow is not within the level of detection of the OCT-A device, they may not be visible with this technique,[30] which might explain why we were unable to find polyps in some of our suspected cases. In fact, OCT angiograms alone have been shown to have lower sensitivity in detecting polyps, but the detection rate increases when a *fusion* image is reviewed.[35]

In addition to vascular complications, we also analyzed the nevi vascularization at the level of the CC and the choroid, but in some cases the shadowing effect and signal absorption by the melanin prevented the acquisition of high-quality images. At the level of the CC, the majority of CN were isorreflective demonstrating a normal plexus, but CN with greater thickness, compressing the choriocapillaris, appeared hyporreflective. Several studies[4,5,24,36] that have analyzed the intrinsic vascular features of choroid tumors demonstrated variable results. We think that the discrepancy between studies may be explained by the different levels in which the nevi were analyzed (choriocapillaris/choroid) as well as the difference in thickness and pigmentation of the tumors.

Thus, it seems that current OCT-A equipment still have limited capacity to assess intrinsic vascularization of choroidal tumors. The microcirculation of CN is similar to the surrounding vessels, but in choroidal melanoma more complex vascular patterns are present.[5] We believe that future developments will enable better visualization of lesions located at the periphery, as well as better identification of deeper structures, allowing for recognition of those patterns. Meanwhile, we consider that fundus photography, EDI-OCT, FAF and US are indispensable tools to monitor CN, as these lesions can complicate with subretinal fluid, neovascularization or even transform into melanoma. Although angiography (FA/ICGA) is still the gold standard technique to diagnose neovascularization, we think that OCT-A should be incorporated into routine evaluation of longstanding nevi with large PEDs and/or recent onset of exudation.

Our study is limited by its retrospective nature and the reduced number of cases. In addition, the use of current OCT-A devices to visualize CN has also some intrinsic limitations, related to the depth of the lesions, the limited field of view, the inability to show leakage and the presence of motion and projection artifacts.

CONCLUSION

In conclusion, we found that OCT-A may be a useful and safe complementary imaging technique to monitor choroidal nevi, located at the posterior pole, with thickness less than 1.5 mm. Future prospective studies will be needed to identify on OCT-A imaging, biomarkers of choroidal nevi activity, in order to distinguish vascular complications from malignant transformation and define a therapeutic strategy.

REFERENCES

1. M. Materin AS. Benign melanocytic tumors of the uvea. In: B. Damato; A. Singh, ed. *Clinical Ophthalmic Oncology*. Second ed. Berlin: Springer; 2014:45-46.

2. Cl S, Furuta M, Mashayekhi A, et al. Visual acuity in 3422 consecutive eyes with choroidal nevus . 2019;125(11):1-2. doi:10.1001/archopht.125.11.1501
3. Qiu M, Cl S. Choroidal Nevus in the United States Adult Population : Racial Disparities and Associated Factors in the National Health and Nutrition Examination Survey . 2019;122(10):9-10. doi:10.1016/j.ophtha.2015.06.008
4. Cennamo G, Romano MR, Breve MA, et al. Evaluation of choroidal tumors with optical coherence tomography : enhanced depth imaging and features. *Nat Publ Gr*. 2017:1-10. doi:10.1038/eye.2017.14
5. Toledo JJ, Asencio-duran M, García-martinez JR, López-gaona A. Use of OCT Angiography in Choroidal Melanocytic Tumors. 2017;2017.
6. Carlo TE De, Romano A, Waheed NK, Duker JS. A review of optical coherence tomography angiography (OCTA). 2015:1-15. doi:10.1186/s40942-015-0005-8
7. Su S, Kaliki S, Cl S, Sr F, Sa H, Ja S. Enhanced depth imaging optical coherence tomography of choroidal nevus in 104 cases . 2019;119(5):10-11. doi:10.1016/j.ophtha.2011.11.001
8. Cl S, Kaliki S, Rojanaporn D, Sr F, Ja S. Enhanced depth imaging optical coherence tomography of small choroidal melanoma : comparison with choroidal nevus . 2019;130(7). doi:10.1001/archophthalmol.2012.1135
9. Collaborative Ocular Melanoma Study Group. Comparison of Clinical, Echographic, and Histopathological Measurements From Eyes With Medium-Sized Choroidal Melanoma in the Collaborative Ocular Melanoma Study. *Arch Ophthalmol*. 2003;121(8):1163. doi:10.1001/archopht.121.8.1163
10. Shields C, Manalac J, Saktanasate J, Shields J, Das C. Review of spectral domain enhanced depth imaging optical coherence tomography of tumors of the choroid. *Indian J Ophthalmol*. 2015;63(2):117. doi:10.4103/0301-4738.154377
11. Service OO, Hospital WE. CHOROIDAL NEVUS IMAGING FEATURES IN 3 , 806 CASES AND RISK FACTORS FOR TRANSFORMATION INTO MELANOMA IN 2 , 355 CASES : The 2020 Taylor R . Smith and Victor T . Curtin. 2020:2018-2019. doi:10.1097/IAE.0000000000002440
12. Age-Related Eye Disease Study Research Group. The Age-Related Eye Disease Study (AREDS): design implications. AREDS report no. 1. *Control Clin Trials*. 1999;20(6):573-600. http://www.ncbi.nlm.nih.gov/pubmed/10588299. Accessed October 13, 2019.
13. Sarks JP, Sarks SH, Killingsworth MC. Evolution of soft drusen in age-related macular degeneration. *Eye (Lond)*. 1994;8 (Pt 3)(3):269-283. doi:10.1038/eye.1994.57
14. Nassisi M, Tepelus T, Mg N, Sr S. Choriocapillaris flow impairment predicts the development and enlargement of drusen . 2019:1-2. doi:10.1007/s00417-019-04403-1
15. Lee J, Byeon SH. PREVALENCE AND CLINICAL CHARACTERISTICS OF PACHYDRUSEN IN POLYPOIDAL CHOROIDAL VASCULOPATHY: Multimodal Image Study. *Retina*. 2019;39(4):670-678. doi:10.1097/IAE.0000000000002019
16. Dansingani KK, Balaratnasingam C, Naysan J, Freund KB. EN FACE IMAGING OF PACHYCHOROID SPECTRUM DISORDERS WITH SWEPT-SOURCE OPTICAL COHERENCE TOMOGRAPHY. *Retina*. 2016;36(3):499-516. doi:10.1097/IAE.0000000000000742
17. Roquet W, Roudot-Thoraval F, Coscas G, Soubrane G. Clinical features of drusenoid pigment epithelial detachment in age related macular degeneration. *Br J Ophthalmol*. 2004;88(5):638-642. doi:10.1136/bjo.2003.017632
18. Zografos L, Mantel I, Schalenbourg A. Subretinal choroidal neovascularization associated with choroidal nevus. *Eur J Ophthalmol*. 2004;14(2):123-131. doi:10.1177/112067210401400207
19. Vp P, Nogueira V, Hay G, et al. Choroidal naevi complicated by choroidal neovascular membrane and outer retinal tubulation . 2019:1-2. doi:10.1136/bjophthalmol-2013-303234
20. Callanan DG, Lewis ML, Byrne SF, Gass JD. Choroidal neovascularization associated with choroidal nevi. *Arch Ophthalmol (Chicago, Ill 1960)*. 1993;111(6):789-794. doi:10.1001/archopht.1993.01090060077026
21. Gupta MP, Rusu I, Seidman C, Orlin A, D'Amico DJ, Kiss S. Pachychoroid neovasculopathy in extramacular choroidal neovascularization. *Clin Ophthalmol*. 2016;10:1275-1282. doi:10.2147/OPTH.S105080
22. Te DC, Romano A, Nk W, Js D. A review of optical coherence tomography angiography (OCTA). 2019:9-10. doi:10.1186/s40942-015-0005-8

23. Pellegrini M, Corvi F, Say EAT, Shields CL, Staurenghi G. OPTICAL COHERENCE TOMOGRAPHY ANGIOGRAPHY FEATURES OF CHOROIDAL NEOVASCULARIZATION ASSOCIATED WITH CHOROIDAL NEVUS. *Retina*. 2018;38(7):1338-1346. doi:10.1097/IAE.0000000000001730
24. C GF, F PI. Is optical coherence tomography angiography helpful in the differential diagnosis of choroidal nevus versus melanoma ? 2019:1-2. doi:10.1177/1120672119851768
25. De Salvo G, Vaz-Pereira S, Sehmi KS, Andrews RM, Sagoo MS. Spectral-domain optical coherence tomography of polypoidal choroidal vasculopathy associated with benign choroidal nevus. *Ophthalmic Surg Lasers Imaging Retin*. 2015;46(10):1062-1064. doi:10.3928/23258160-20151027-15
26. Clinic SR, Hospital SE, Sciences B, et al. POLYPOIDAL CHOROIDAL VASCULOPATHY SECONDARY TO A STABLE CHOROIDAL NEVUS . 2019;10(3). doi:10.1097/ICB.0000000000000233
27. Wong JG, Smith JB. Photodynamic therapy for polypoidal choroidal vasculopathy secondary to choroidal nevus. 2017:51-54.
28. Peiretti E, Pozzoni MC, Fossarello M, Spaide RF. POLYPOIDAL CHOROIDAL VASCULOPATHY IN ASSOCIATION WITH CHOROIDAL NEVUS. *Retin Cases Brief Rep*. 2009;3(1):12-14. doi:10.1097/icb.0b013e318166bd70
29. Yannuzzi LA, Sorenson J, Spaide RF, Lipson B. Idiopathic polypoidal choroidal vasculopathy (IPCV). 1990. *Retina*. 2012;32 Suppl 1:1-8. http://www.ncbi.nlm.nih.gov/pubmed/22451948. Accessed October 13, 2019.
30. Kumar A, Kumawat D, M DS, Gagrani M. Polypoidal choroidal vasculopathy : a comprehensive clinical update. 2019:1-26. doi:10.1177/https
31. De Salvo G, Vaz-Pereira S, Sehmi KS, Andrews RM, Sagoo MS. Spectral-Domain Optical Coherence Tomography of Polypoidal Choroidal Vasculopathy Associated With Benign Choroidal Nevus. *Ophthalmic Surgery, Lasers Imaging Retin*. 2015;46(10):1062-1064. doi:10.3928/23258160-20151027-15
32. De Salvo G, Vaz-Pereira S, Keane PA, Tufail A, Liew G. Sensitivity and Specificity of Spectral-Domain Optical Coherence Tomography in Detecting Idiopathic Polypoidal Choroidal Vasculopathy. *Am J Ophthalmol*. 2014;158(6):1228-1238.e1. doi:10.1016/j.ajo.2014.08.025
33. Chi Y-T, Yang C-H, Cheng C-K. Optical Coherence Tomography Angiography for Assessment of the 3-Dimensional Structures of Polypoidal Choroidal Vasculopathy. *JAMA Ophthalmol*. 2017;135(12):1310-1316. doi:10.1001/jamaophthalmol.2017.4360
34. Chan SY, Wang Q, Wang YX, Shi XH, Jonas JB, Wei W Bin. POLYPOIDAL CHOROIDAL VASCULOPATHY UPON OPTICAL COHERENCE TOMOGRAPHIC ANGIOGRAPHY. *Retina*. 2018;38(6):1187-1194. doi:10.1097/IAE.0000000000001702
35. De Carlo TE, Kokame GT, Kaneko KN, Lian R, Lai JC, Wee R. Sensitivity and specificity of detecting polypoidal choroidal vasculopathy with en face optical coherence tomography and optical coherence tomography angiography. *Retina*. 2019;39(7):1343-1352. doi:10.1097/IAE.0000000000002139
36. Ghassemi F, Mirshahi R, Fadakar K, Sabour S. Optical coherence tomography angiography in choroidal melanoma and nevus. *Clin Ophthalmol*. 2018;12:207-214. doi:10.2147/OPTH.S148897

CONTACT

Susana Henriques
Hospital Prof. Doutor Fernando Fonseca E.P.E . IC 19
2720-276 AmadoraIC19 – Venteira
E-mail: susanapintohenriques@gmail.com

Sem conflito de interesses.
Sem publicação prévia.